

Supplementary Information

Effect of Charge Density on the Viscoelasticity and Underwater Adhesion of Entangled Complex Coacervates from Semi-Rigid Polysaccharides

Maxime Precheur¹, Ali Kanan¹, Alexei Dmitrievitsj Filippov¹, Kylian Virieux², Stéphane Trombotto², Fouzia Boulmedais¹, Mehdi Vahdati^{1,*}

1. University of Strasbourg, CNRS, Institut Charles Sadron, UPR22, 67200 Strasbourg, France
2. Ingénierie des Matériaux Polymères, UMR 5223, Université Claude Bernard Lyon 1, CNRS, INSA Lyon, Université Jean Monnet Saint-Etienne, F-69622 Villeurbanne, France.

*Corresponding author: mehdi.vahdati@ics-cnrs.unistra.fr

Determination of degree of deacetylation (DD) and degree of substitution (DS) of chitosans by Proton Nuclear Magnetic Resonance Spectroscopy (¹H NMR)

¹H NMR spectra were recorded on an AV300 Bruker (300 MHz) spectrometer at ambient temperature. Samples were dissolved at 10 mg/mL in D₂O with 5 uL HCl (12 N) and transferred to 5 mm NMR tubes. Trimethylsilyl-3-propionic-2,2,3,3-D₄ acid sodium salt (Sigma-Aldrich, France) was used as an internal reference. The Bruker Topspin software was used for the analysis of spectra (Bruker, version 3.6). The DD of chitosans was determined according to the method described by Hirai et al.¹ The degree of substitution (DS) of chitosan by butyric anhydride group was determined taking into account integrals of the CH₃ signal of butyric group at 0.9 ppm and the H2 to H6 signals of pyranose units from 4.4 to 2.8 ppm.

Determination of average molar masses of chitosan by Size Exclusion Chromatography (SEC)

The weight- and number-average molar masses (M_w and M_n) of chitosan, as well as its dispersity ($\mathcal{D} = M_w/M_n$), were quantified using size exclusion chromatography (SEC). Chitosan samples were dissolved at 1 mg/mL in a 0.2 M acetic acid / 0.15 M ammonium acetate buffer (pH 4.5) and allowed to hydrate for at least 18 h at room temperature before analysis. The resulting solutions were passed through 0.45 μ m CME membrane filters (Millipore, USA). SEC separation was

achieved with two TSK G2500PW and G6000PW columns arranged in series (Tosoh Bioscience, Japan). Detection was carried out using an online differential refractometer (Optilab T-rex, Wyatt Technology, USA) coupled online with a MALLS detector (Dawn Heleos II, Wyatt Technology, USA). The eluent consisted of the same buffer, degassed and filtered through a 0.10 μm membrane (Millipore, USA), and was delivered at 0.5 mL/min. Each run involved a 100 μL injection volume. The refractive index increments (dn/dc) used for calculation were 0.198 mL/g for native chitosan, determined following Schatz et al.² and 0.190 mL/g for the butyrylated derivative, measured using the procedure described by Nguyen et al.³ Data processing and molar mass calculations were performed with ASTRA 6.1 (Wyatt Technology, USA)

Hyaluronic acid molecular weight determination via SEC

The number- and weight-average molar masses (M_n and M_w) of hyaluronic acid (HA) were measured by size exclusion chromatography (SEC). HA was dissolved at 2 $\text{mg}\cdot\text{mL}^{-1}$ in Milli-Q water containing 0.1 M NaNO_3 and left to equilibrate for at least 24 h at room temperature. Prior to injection, the solutions were filtered through 0.45 μm hydrophilic PTFE membranes (Millex-LCR, Millipore). SEC was carried out using a series of four columns (Shodex OH-Pak SB-802.5 HQ, SB-804 HQ, SB-806 HQ and SB-807 HQ, Showa Denko). Detection was performed with a differential refractometer (Optilab T-rex, Wyatt Technology) connected in-line with a multi-angle light scattering detector (Dawn Heleos II, Wyatt Technology). The mobile phase consisted of Milli-Q water containing 0.1 M NaNO_3 , filtered through a 0.10 μm membrane, and delivered at 0.5 $\text{mL}\cdot\text{min}^{-1}$. Each analysis used a 100 μL injection. A refractive index increment (dn/dc) of 0.145 $\text{mL}\cdot\text{g}^{-1}$ was applied for molar mass determination. Chromatographic and MALS data were processed using ASTRA 7.1 (Wyatt Technology).

Preparation of CHI-HA complex coacervates

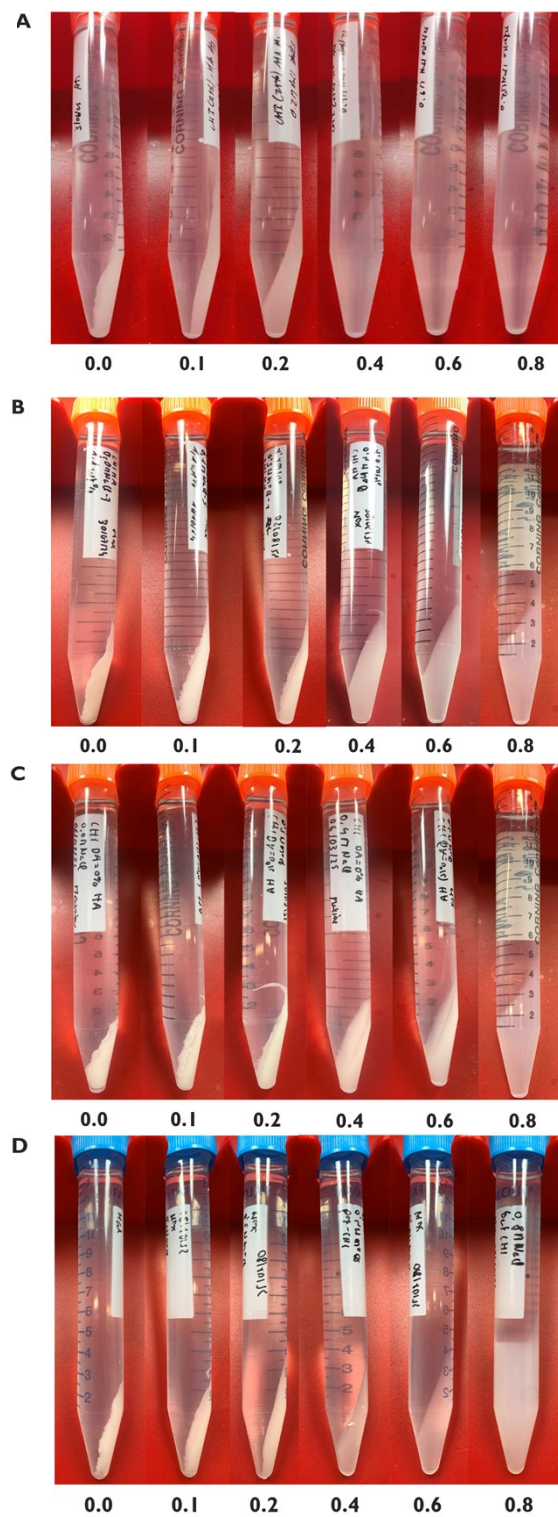


Figure S1. Images of (A) HA-CHI-71, (B) HA-CHI-88, (C) HA-CHI-98, (D) HA-*but*-CHI-88 complex coacervates after preparation.

Thermogravimetric analysis (TGA)

As detailed in **Figure S1**, the water content of the samples was determined from the mass loss observed during the isothermal step at 150 °C. The polymer content was determined from the mass loss occurring between 150 °C and 700 °C. The residual mass remaining at 700 °C was attributed to the total salt content, as both the counterions and the added salt were NaCl. To deconvolute the TGA data, reference thermograms of CHIs and HA were recorded individually. Analysis of these reference materials revealed that 97 wt% of CHI-71, 96 wt% of CHI-88, 98 wt% of CHI-98, 98 wt% of *but*-CHI-88 and 84 wt% of HA were degraded between 150°C and 700°C. The experimental error of the TGA measurements is below 1.0 wt%. To account for changes in both the volume fraction and the density of the supernatant (SN) and complex coacervate (CC), the mass concentrations (w in wt%) for PE and NaCl calculated below were converted to molar concentrations using the following calculations:

The total volume V_{tot} , the mass of the supernatants m_{SN} , the total mass m_{tot} , and the density of the supernatants d_{SN} were measured experimentally. From these values, the volume of the complex coacervates V_{CC} and supernatant V_{SN} , as well as the mass of the complex coacervates m_{CC} , were calculated. The molar concentration of HA in the coacervate phase was then determined as:

$$[HA] = \frac{n_{HA}}{V_{CC}} = \frac{m_{HA}}{M_{HA} * V_{CC}} \quad (1)$$

where the mass of HA, m_{HA} , is related to the total polymer mass m_{PE} and the HA:CHI mass ratio, a (determined by the formulation), as follows:

$$m_{HA} = m_{PE} - m_{CHI} = m_{PE} - \frac{m_{HA}}{a}$$

$$\Rightarrow m_{HA} = \frac{m_{PE}}{\left(1 + \frac{1}{a}\right)} \quad (2)$$

The total polymer mass, m_{PE} , can be related to the mass concentration of PE (w_{PE}) and the mass of the complex coacervate, m_{CC} , by:

$$m_{PE} = w_{PE} * m_{CC} \quad (3)$$

Finally, combining equations (1)-(3) gives:

$$[HA] = \frac{w_{PE} * m_{CC}}{M_{HA} * V_{CC} * \left(1 + \frac{1}{a}\right)} \quad (4)$$

The same procedure was applied to determine CHI concentration, and the total polymer

concentration was obtained as:

$$[PE] = [HA] + [CHI] \quad (5)$$

Molar concentrations of NaCl were calculated analogously by replacing w_{PE} and M_{HA} with w_{NaCl} and M_{NaCl} , respectively. The same calculations were also applied to the supernatant phase by substituting V_{CC} and m_{CC} with V_{SN} and m_{SN} in the above calculations.

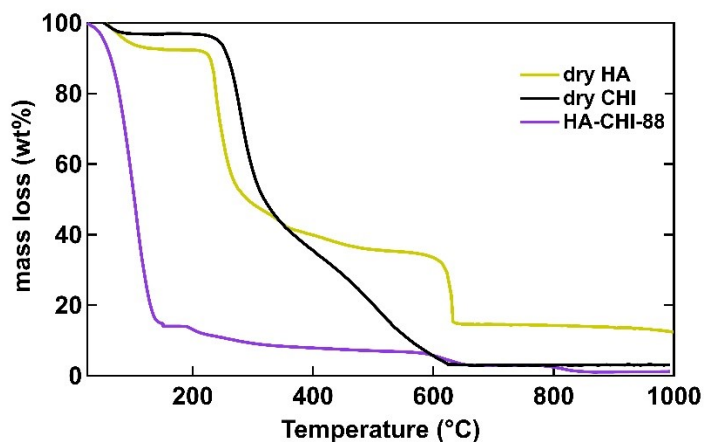


Figure S2. Thermogravimetric behavior of a complex CC (0.4 M NaCl and HA-CHI-88), compared with the individual components HA and typical CHI-88

Phase behavior

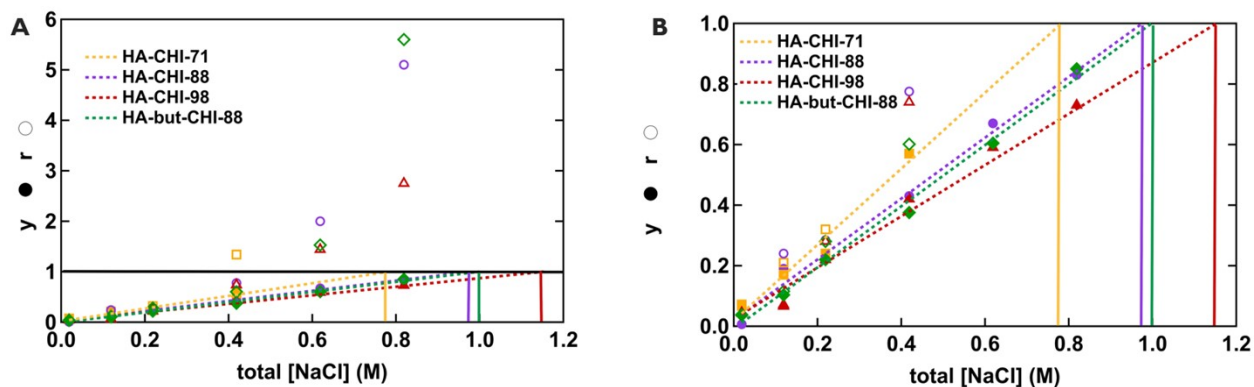


Figure S3. Doping level, y , and the molar ratio between salts and polyelectrolytes in the coacervate phase, r . The colored lines mark the CSC as predicted from $y=1$.

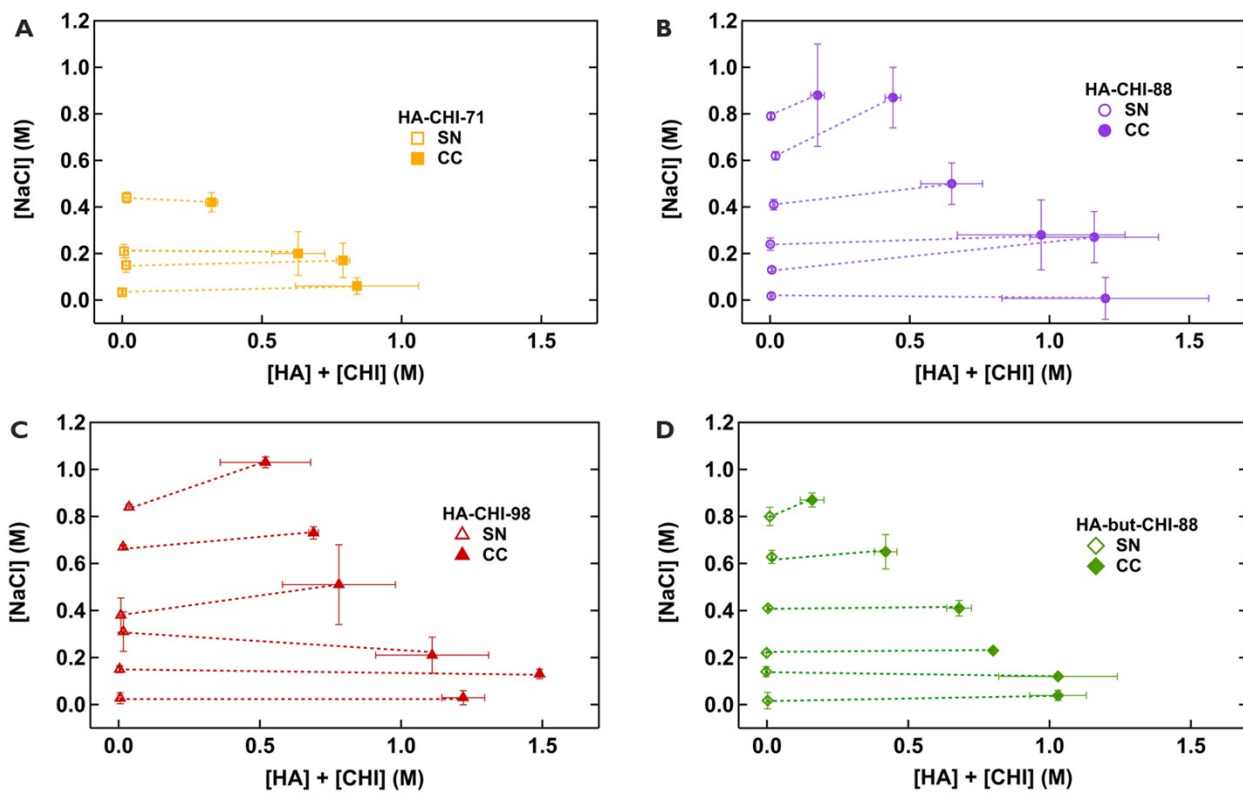


Figure S4. Individual phase diagrams with tie lines of (A) HA-CHI-71, (B) HA-CHI-88, (C) HA-CHI-98, and (D) HA-but-CHI-88 complex coacervates as a function of added NaCl in M.

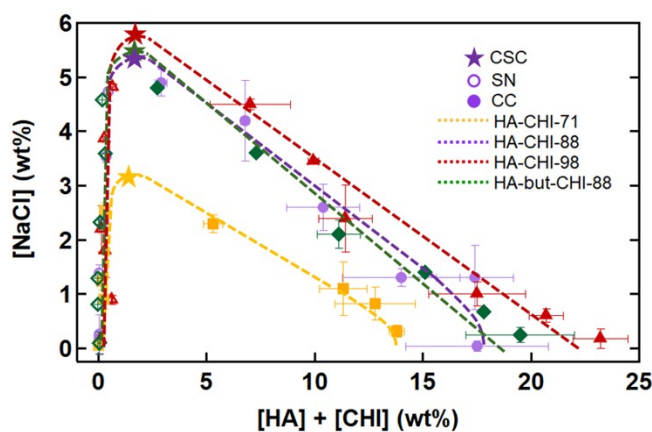


Figure S5. Phase diagram of the HA-CHI complex coacervates as a function of added NaCl in wt%

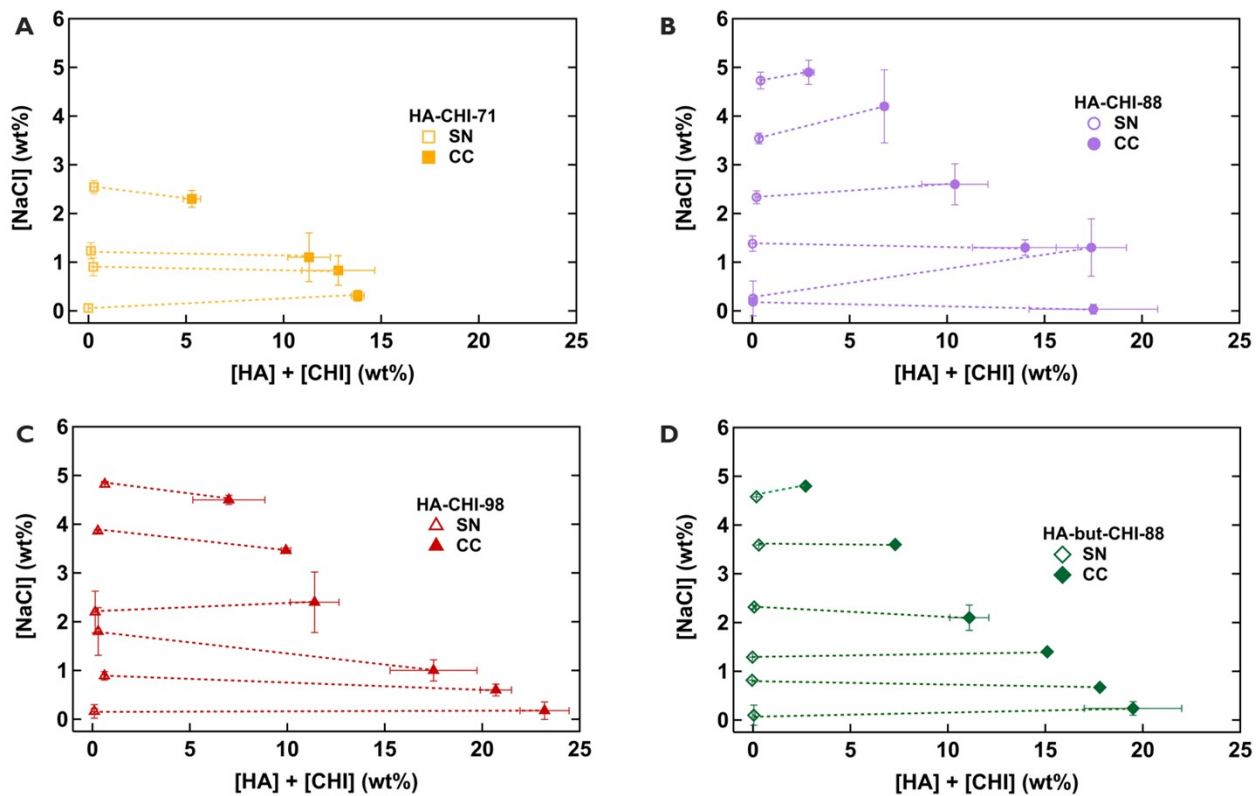


Figure S6. Individual phase diagrams with tie lines of (A) HA-CHI-71, (B) HA-CHI-88, (C) HA-CHI-98, and (D) HA-but-CHI-88 complex coacervates as a function of added NaCl in wt%.

Viscoelasticity of HA-CHI complex and time-salt superposition

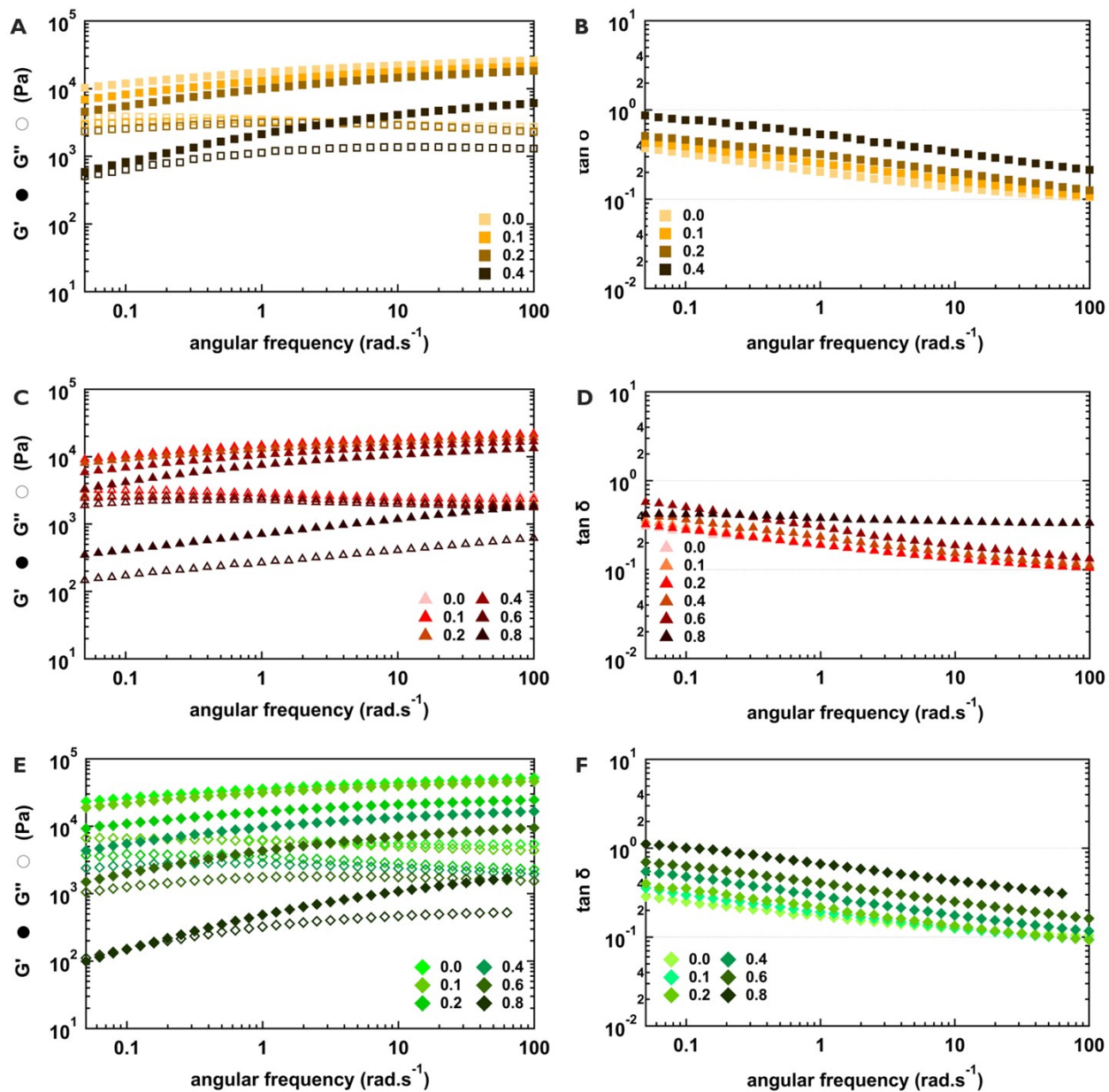


Figure S7. Linear viscoelastic properties of the (A) and (B) HA-CHI-71, (C) and (D) HA-CHI-98, (E) and (F) HA-but-CHI-88 complex coacervates prepared at 37°C: storage modulus (G'), loss modulus (G''), and loss factor, $\tan(\delta) = G''/G'$ as a function of angular frequency.

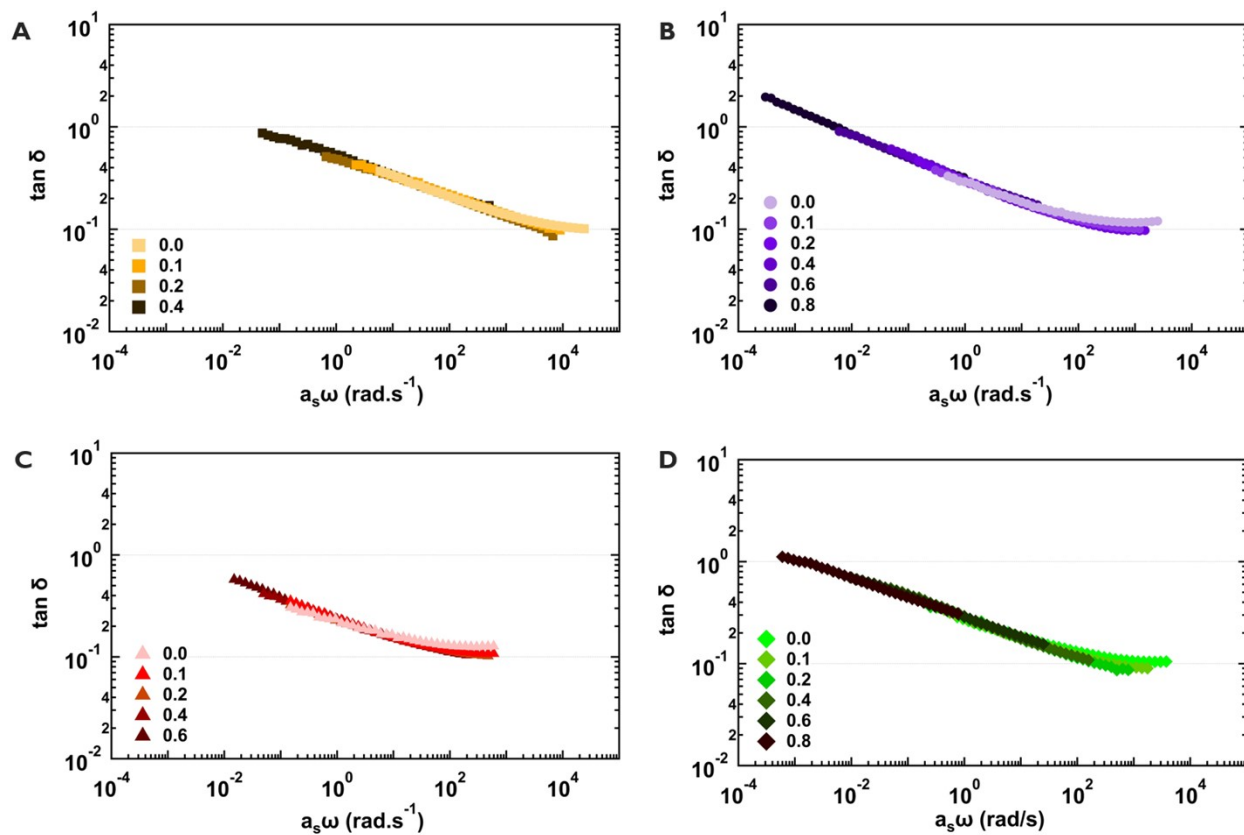


Figure S8. Rescaled viscoelastic loss factor of (A) HA-CHI-71, (B) HA-CHI-88, (C) HA-CHI-98, (D) HA-*but*-CHI-88 complex coacervates using time-salt superposition (TSS), taking the 0.4 M NaCl sample as the reference for each series.

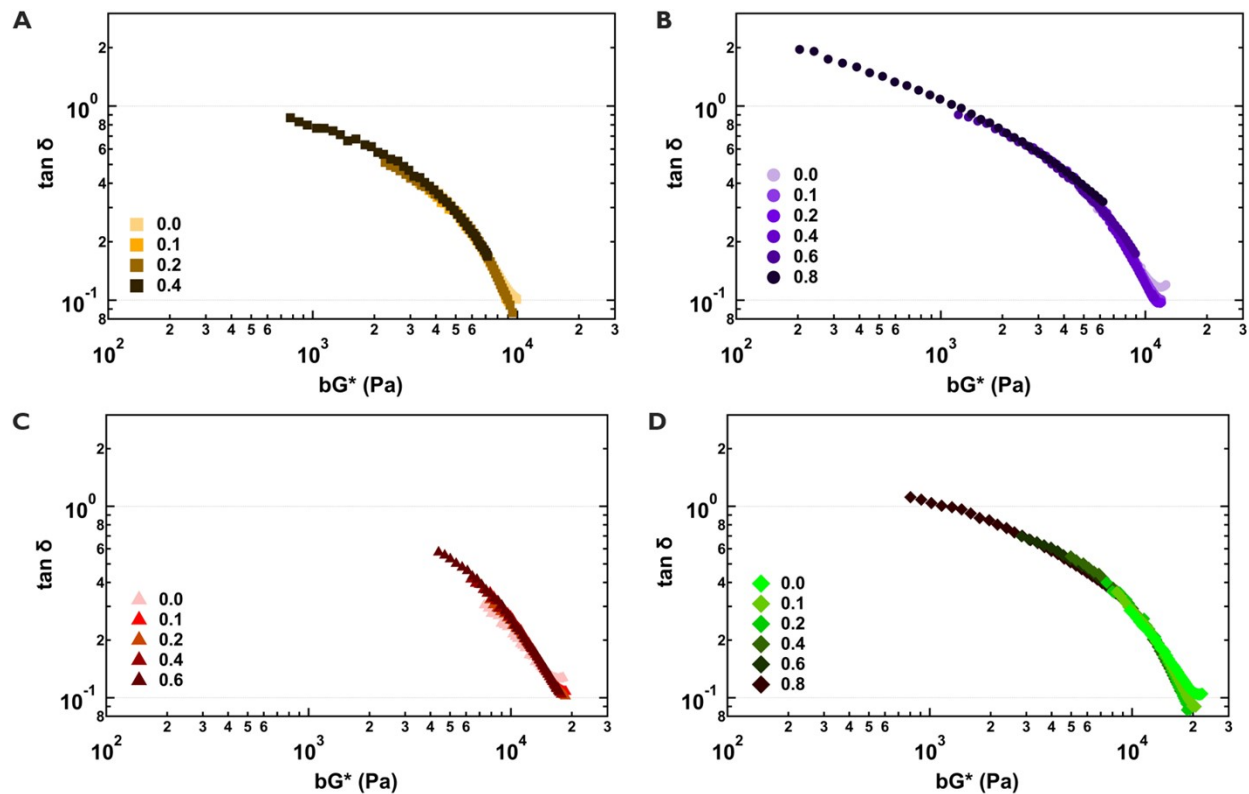
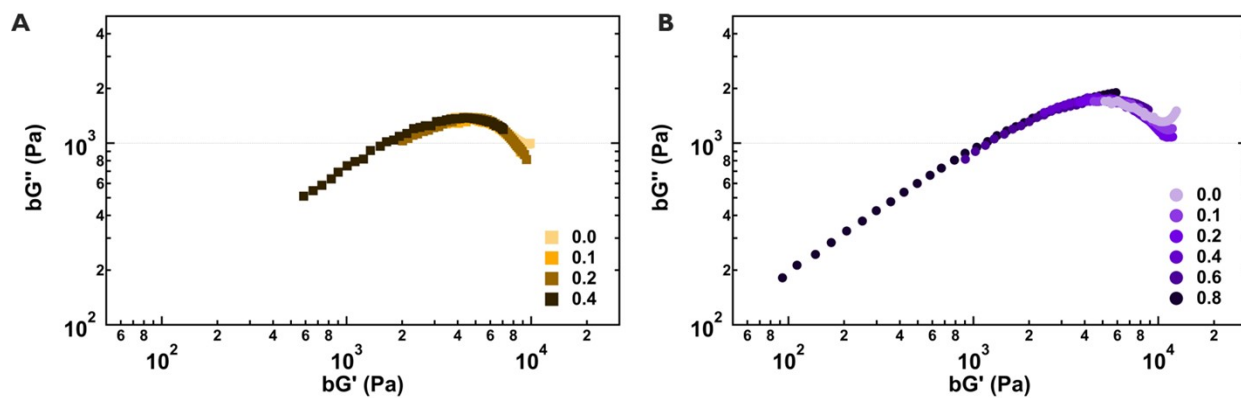


Figure S9. Van Gurp–Palmen plots that confirm the validity of a time–salt superposition (TSS) of (A) HA-CHI-71, (B) HA-CHI-88, (C) HA-CHI-98, (D) HA-*but*-CHI-88 complex coacervates.



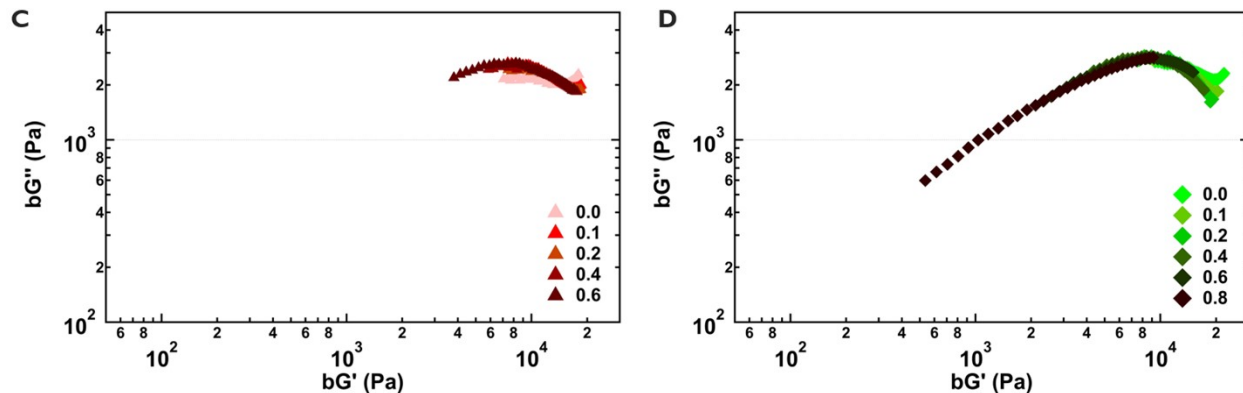
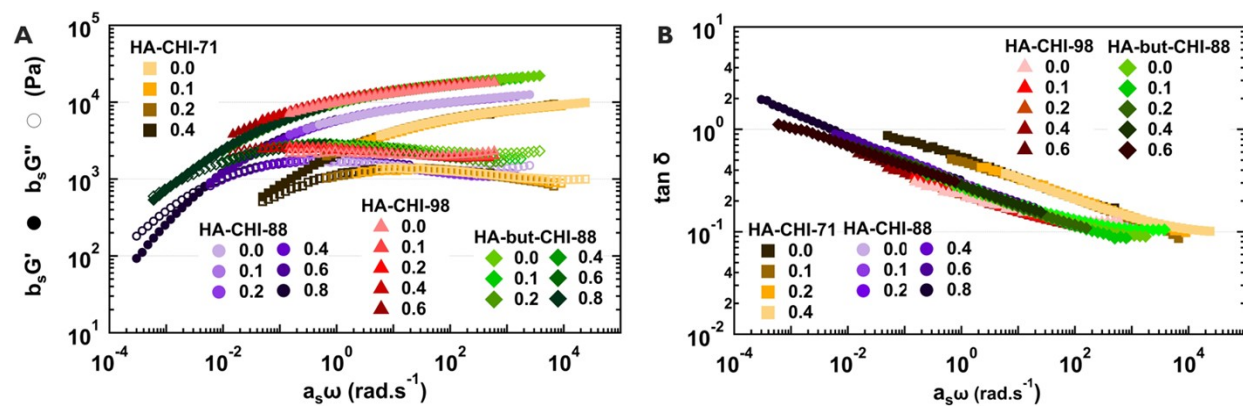


Figure S10. Cole-Cole plots that confirm the validity of a time-salt superposition (TSS) of (A) HA-CHI-71, (B) HA-CHI-88, (C) HA-CHI-98, (D) HA-*but*-CHI-88 complex coacervates.



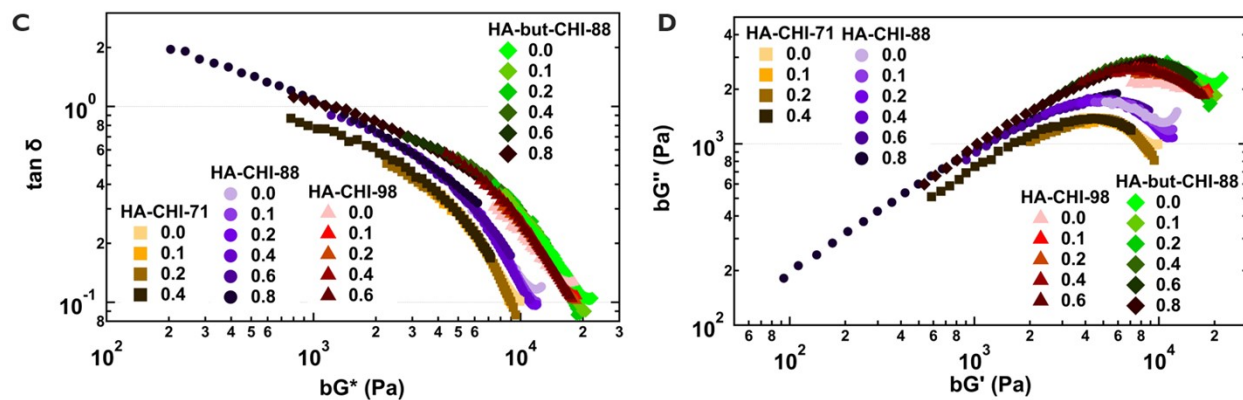


Figure S11. (A) Rescaled dynamic modulus, (B) loss factors, (C) Van Gorp–Palmen plots, and (D) Cole-Cole plots of all complex coacervates for time-salt superposition (TSS), taking the 0.4 M NaCl sample within each series as the reference.

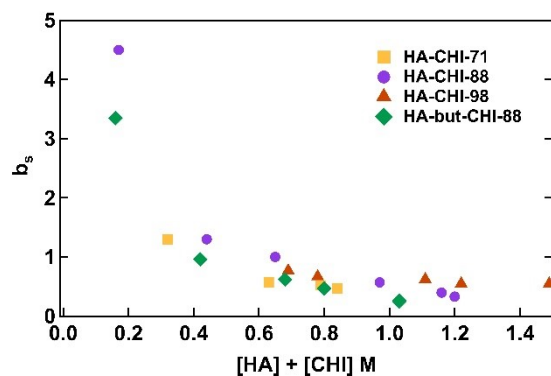


Figure S12. Vertical shift factors b_s as a function of the polymer concentration.

Time-salt-charge density/hydrophobicity superposition

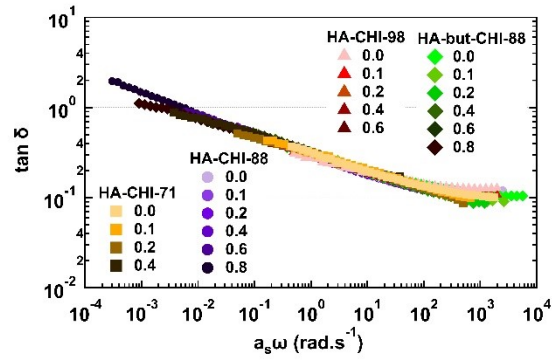


Figure S13. Rescaled loss factors of all complex coacervates for time–salt–charge density superposition (TSCDS), taking the 0.4 M NaCl sample of HA-CHI-88 system as the reference.

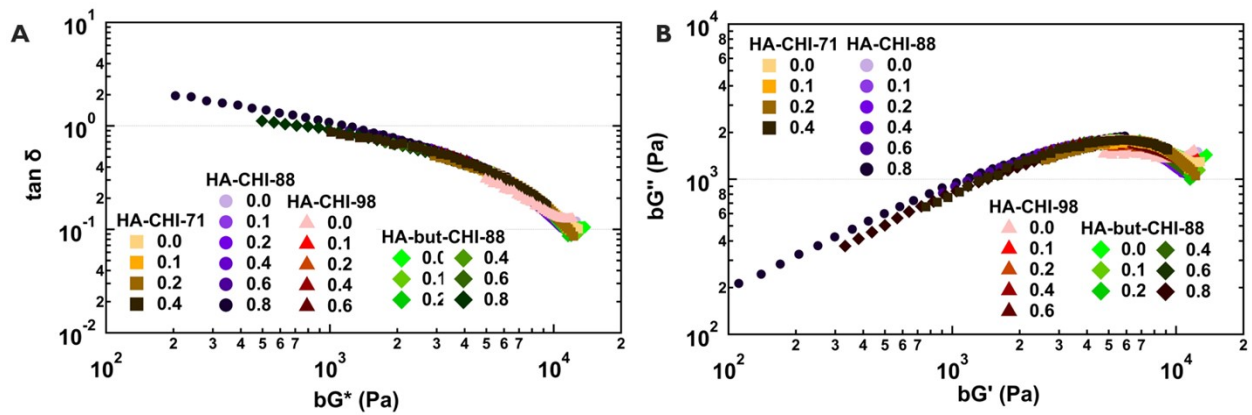


Figure S14. (A) Van Gurp–Palmen plots, and (B) Cole-Cole plots of all complex coacervates for time–salt–charge density superposition (TSCDS), taking the 0.4 M NaCl sample of HA-CHI-88 system as the reference.

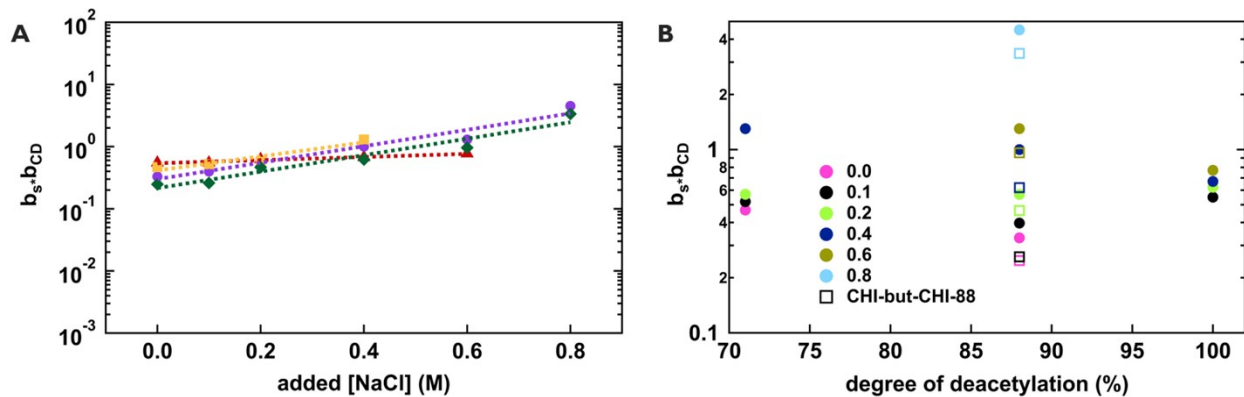


Figure S15. Vertical shift factors $b_s \cdot b_{CD}$ as a function of (A) the added salt concentration and (B) CHI's degree of deacetylation.

Underwater adhesion

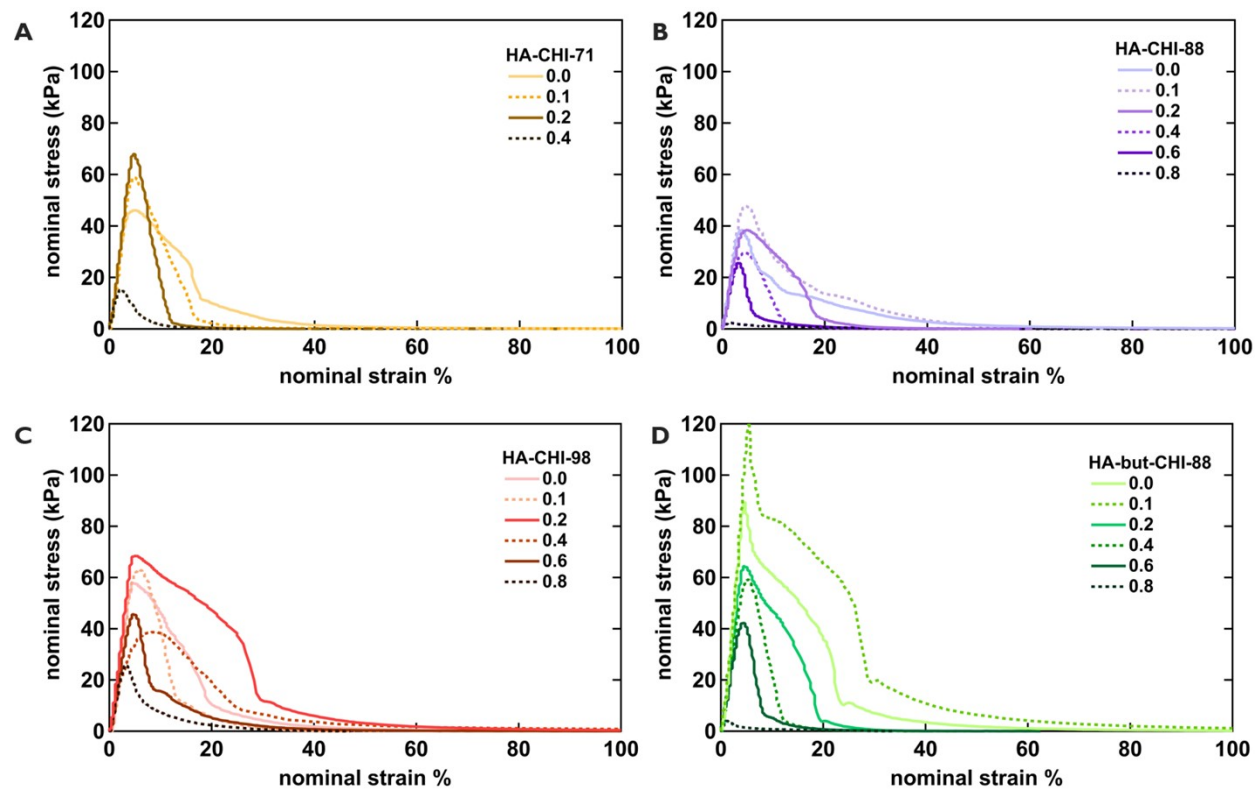


Figure S16. Representative stress-strain curves for (A) HA-CHI-71, (B) HA-CHI-88, (C) HA-CHI-98, and (D) HA-but-CHI-88.

References

- 1 A. Hirai, H. Odani and A. Nakajima, *Polymer Bulletin*, 1991, **26**, 87–94.
- 2 C. Schatz, C. Viton, T. Delair, C. Pichot and A. Domard, *Biomacromolecules*, 2003, **4**, 641–648.
- 3 S. Nguyen, F. Winnik and M. Buschmann, *Carbohydr Polym*, 2009, **75**, 528–533.
- 4 M. Vahdati, F. J. Cedano-Serrano, C. Creton and D. Hourdet, *ACS Appl Polym Mater*, 2020, **2**, 3397–3410.